# Quantum-Chemical, IR, NMR, and X-ray Diffraction Studies on 2-(4-Chlorophenyl)-1-methyl-1*H*-benzo[*d*]imidazole

**NAMIK ÖZDEMİR,[1] BİLGE EREN,[2] MUHARREM DİNÇER,[1] YUNUS BEKDEMİR[3]**

[1]*Department of Physics, Faculty of Arts and Sciences, Ondokuz Mayıs University, 55139 Kurupelit, Samsun, Turkey*

[2]*Department of Chemistry, Faculty of Arts and Sciences, Bilecik University 11100, Bilecik, Turkey*

[3]*Department of Chemistry, Faculty of Arts and Sciences, Ondokuz Mayıs University, 55139 Kurupelit, Samsun, Turkey*

*Received 24 October 2009; accepted 25 February 2010*
*Published online 27 July 2010 in Wiley Online Library (wileyonlinelibrary.com).*
*DOI 10.1002/qua.22697*

**ABSTRACT:** The title molecule, 2-(4-chlorophenyl)-1-methyl-1*H*-benzo[*d*]imidazole ($C_{14}H_{11}ClN_2$), was prepared and characterized by $^1$H NMR, $^{13}$C NMR, IR, and single-crystal X-ray diffraction. The molecular geometry, vibrational frequencies, and gauge including atomic orbital (GIAO) $^1$H and $^{13}$C NMR chemical shift values of the title compound in the ground state have been calculated by using the Hartree-Fock (HF) and density functional theory (DFT/B3LYP) method with 6-31G(d) basis sets, and compared with the experimental data. The calculated results show that the optimized geometries can well reproduce the crystal structural parameters, and the theoretical vibrational frequencies and GIAO $^1$H and $^{13}$C NMR chemical shifts show good agreement with experimental values. The energetic behavior of the title compound in solvent media has been examined using B3LYP method with the 6-31G(d) basis set by applying the Onsager and the polarizable continuum model (PCM). Besides, molecular electrostatic potential (MEP), frontier molecular orbitals (FMO) analysis, and nonlinear optical (NLO) properties of the title compound were investigated by theoretical calculations.  Int J Quantum Chem 111: 3112–3124, 2011

**Key words:** 2-(4-chlorophenyl)-1-methyl-1*H*-benzo[*d*]imidazole; crystal structure; IR and NMR spectroscopy; *ab initio* calculations; nonlinear optical (NLO) properties

*Correspondence to:* N. Özdemir; e-mail: namiko@omu.edu.tr
Contract grant sponsor: Research Centre of Ondokuz Mayıs University, Project No: F-461.

## Introduction

Benzimidazoles are regarded as a promising class of bioactive heterocyclic compounds that exhibit a range of biological activities. Because of its synthetic utility and broad range of pharmacological activities, the benzimidazole nucleus is an important heterocyclic ring. Specifically, this nucleus is a constituent of vitamin-B12 [1]. This ring system is present in numerous antioxidant [2–4], antiparasitic [5, 6], antihelmintics [7], antiproliferative [8], anti-HIV [9], anticonvulsant [10], antiinflammatory [11–14], antihypertensive [15, 16], antineoplastic [17, 18], antitrichinellosis [19], antimicrobial [20, 21], antihistaminic [22], antifungal [23, 24], and anticancer [25] activities. Owing to the immense importance and varied bioactivities exhibited by benzimidazoles, efforts have been made from time to time to generate libraries of these compounds and screened them for potential biological activities.

It is also well known that imidazole-containing molecules can easily coordinate to metal ions as well as act as hydrogen-bond acceptors or donors in supramolecular assembly reactions [26, 27], and thus, their chemistry has been investigated extensively in coordination chemistry [28, 29]. The inclusion of benzimidazole functional group can lead to different coordination modes and may play a crucial role in the construction of supramolecular compounds driven by hydrogen-bonding interactions [30–32]. In addition, benzimidazole-based organic ligands and their metal complexes continue to attract interest as components in homogeneous catalysis [33]. These different applications have attracted many experimentalists and theorist to investigate the spectroscopic and structural properties of benzimidazole [34–36] and some of its derivatives [37].

Looking at the importance of benzimidazole nucleus, it was thought that it would be worthwhile to design and synthesize some new benzimidazole derivatives. In this study, we present results of a detailed investigation of the synthesis and structural characterization of the title compound using single crystal X-ray diffraction, IR-NMR spectroscopy, and quantum chemical methods. The geometrical parameters, fundamental frequencies and GIAO $^{1}H$ and $^{13}C$ NMR chemical shift values of the title compound in the ground state have been calculated by using the Hartree–Fock (HF) and DFT (B3LYP) methods with 6-31G(d) basis set. These calculations are valuable for providing insight into molecular parameters and the vibrational spectrum and NMR spectrum. The aim of this work is to explore the molecular dynamics and the structural parameters that govern the chemical behavior and to compare predictions made from theory with experimental observations.

## Experimental and Computational Methods

### GENERAL

The melting point was determined with a capillary tube on a digital melting point apparatus (Gallenkamp Electrotermal) and is uncorrected. Reactions under microwave irradiation were performed in a modified domestic microwave oven, BOSCH HMT 812C. Reactions were monitored by thin-layer chromatography (TLC) on silica-gel 60 $F_{254}$ plates (Merck) and an UV lamp. The IR spectrum of the title compound was recorded in the range of 4000−400 $cm^{-1}$ region with a Bruker Vertex 80v FTIR spectrometer using KBr pellets. The $^{1}H$ and $^{13}C$ NMR spectra were recorded with Bruker (400 MHz) spectrometer using TMS as an internal standard and DMSO-$d_6$ as solvent. All the chemicals and solvents used were of analytical grade.

### PREPARATION

The title compound was obtained by condensation of *N*-methyl-*o*-phenylenediamine with the $NaHSO_3$ adduct of 4-chlorophenylbenzaldehyde according to the method described by Ridley and et al[38], but under neat microwave conditions. 4-Chlorophenylbenzaldehyde (5.73 g, 40 mmol) was dissolved in 20 ml ethanol and $NaHSO_3$ (4.16 g, 40 mmol) in 20 ml water was added in portions. The mixture was stirred vigorously an hour in an ice bath. The precipitate was $NaHSO_3$ adduct of 4-chlorophenylbenzaldehyde, filtered as white solid and dried under vacuo (7.52 g, yield: 77%). 1 mmol (0.12 g, 0.117 ml) *N*-methyl-*o*-phenylenediamine and 1 mmol (0.24 g) $NaHSO_3$ adduct of 4-chlorophenylbenzaldehyde were mixed. After adding a few drops of DMF, the mixture was irradiated in a modified domestic microwave oven for 20 min until the reaction was completed according to the TLC data. The mixture was cooled and poured onto ice cold water under vigorous stirring. The precipitate was collected by filtration, washed with water and dried (0.17 g, yield: 70%, m.p. 382–

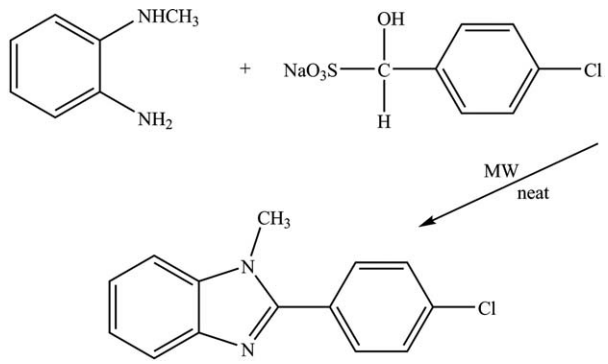


**FIGURE 1.** Formation of the title compound.

383 K). The single crystals suitable for X-ray analysis were obtained by recrystallization from methanol/water. The synthesis pathway of the title compound is shown in Figure 1.

### X-RAY CRYSTALLOGRAPHY

A suitable colorless plate-shaped crystal sample of size 0.80 mm × 0.47 mm × 0.02 mm was chosen for the crystallographic study and then carefully mounted on goniometer of a STOE diffractometer with an IPDS(II) image plate detector. All diffraction measurements were performed at room temperature (296 K) using graphite monochromated Mo K$\alpha$ radiation ($\lambda$ = 0.71073 Å) in $\omega$-scanning mode. The structure was solved by direct methods using SHELXS-97 [39] implemented in WinGX [40] program suit. The refinement was carried out by full-matrix least-squares method on the positional and anisotropic temperature parameters of the nonhydrogen atoms, or equivalently corresponding to 154 crystallographic parameters, using SHELXL-97 [41]. All H atoms were positioned geometrically and treated using a riding model, fixing the bond lengths at 0.93 and 0.96 Å for CH and $CH_3$ atoms, respectively. The displacement parameters of the H atoms were fixed at $U_{iso}(H) = 1.2U_{eq}$ ($1.5U_{eq}$ for methyl) of their parent atoms. Data collection: X-AREA [42] cell refinement: X-AREA, data reduction: X-RED32 [42]. Details of the data collection conditions and parameters of refinement process are given in Table I. The general-purpose crystallographic tool PLATON [43] was used for the structure analysis and presentation of the results.

### COMPUTATIONAL METHODS

The molecular structure of the title compound in the ground state (in vacuo) is optimized by HF and DFT(B3LYP)[44, 45] with the 6-31G(d)[46] basis set. For modeling, the initial guess of the title compound was first obtained from the X-ray coordinates. Then, vibrational frequencies for the optimized molecular structures of the title compound are calculated with these methods and then scaled by 0.8929 and 0.9613 [47], respectively. The geometry of the title compound, together with that of tetramethylsilane (TMS), is fully optimized. $^1$H and $^{13}$C NMR chemical shifts are calculated within GIAO approach [48, 49] applying the same methods and the basis set as that used for geometry optimization. The $^1$H and $^{13}$C NMR chemical shifts are converted to the TMS scale by subtracting the calculated absolute chemical shielding of TMS ($\delta = \Sigma_0 - \Sigma$, where $\delta$ is the chemical shift, $\Sigma$ is the absolute shielding, and $\Sigma_0$ is the absolute shielding of TMS), whose values are 32.52 and 199.79 ppm for HF/6-31G(d) and 32.10 and 189.40 ppm for B3LYP/6-31G(d), respectively. All the calculations are performed by using GaussView molecular visualization program [50] and Gaussian 03 program package [51] on personal computer without specifying any symmetry for the title molecule. The effect of solvent on the theoretical NMR parameters was included using the default model IEF-PCM (Integral-Equation-Formalism Polarizable Continuum Model)[52] provided by Gaussian 03. Dimethylsulfoxide (DMSO) possessing a dielectric constant ($\varepsilon$) of 46.7 was used as solvent. To investigate the total energy and dipole moment behavior of the title compound in solvent media, we have also carried out optimization calculations in three kinds of solvent [$\varepsilon$ = 4.90, chloroform (CHCl3); $\varepsilon$ = 32.63, methanol (CH4O), $\varepsilon$ = 78.39, water (H2O)] at B3LYP/6-31G(d) level using Onsager [53] and Polarizable Continuum Model (PCM)[54–57] methods.

CCDC 733749 contains the supplementary crystallographic data (excluding structure factors) for the structure reported in this article. These data can be obtained free of charge via http://www.ccdc.cam.ac.uk/data_request/cif, by e-mailing data_request@ccdc.cam.ac.uk or by contacting The Cambridge Crystallographic Data Centre, 12, Union Road, Cambridge CB2 1EZ, UK; fax: +44-1223-336033.

## Results and Discussion

### CRYSTAL STRUCTURE

The title compound, an Ortep-3 [58] view of which is shown in Figure 2, crystallizes in the

**TABLE I**

**Crystal data and structure refinement parameters for the title compound.**

| | |
|---|---|
| CCDC deposition no. | 733749 |
| Color/Shape | Colorless/Plate |
| Chemical formula | $C_{14}H_{11}ClN_2$ |
| Formula weight | 242.70 |
| Temperature (K) | 296 |
| Wavelength (Å) | 0.71073 Mo K$\alpha$ |
| Crystal system | Orthorhombic |
| Space group | $P2_12_12_1$ (No. 19) |
| Unit cell parameters | |
| *a*, *b*, *c* (Å) | 7.2035(5), 10.1795(7), 16.4806(9) |
| Volume (Å$^3$) | 1208.49(14) |
| *Z* | 4 |
| Calculated density (Mg/m$^3$) | 1.334 |
| $\mu$ (mm$^{-1}$) | 0.293 |
| Absorption correction | Integration (*X-RED32*) |
| $T_{min}$, $T_{max}$ | 0.8372, 0.9904 |
| $F_{000}$ | 504 |
| Crystal size (mm$^3$) | 0.80 × 0.47 × 0.02 |
| Diffractometer / measurement method | STOE IPDS II / rotation ($\omega$ scan) |
| Index ranges | $-9 \le h \le 9$, $-13 \le k \le 13$, $-21 \le l \le 21$ |
| Theta range for data collection (°) | $2.35 \le \theta \le 27.66$ |
| Measured reflections | 12569 |
| Independent/observed reflections | 2794/1923 |
| $R_{int}$ | 0.0652 |
| Refinement method | Full-matrix least-squares on $F^2$ |
| Data/restraints/parameters | 2794/0/154 |
| Goodness-of-fit on $F^2$ | 1.063 |
| *R* indices [$I > 2\sigma(I)$] | $R_1 = 0.0617$, $wR_2 = 0.1052$ |
| *R* indices (all data) | $R_1 = 0.0979$, $wR_2 = 0.1159$ |
| $\Delta\rho_{max}$, $\Delta\rho_{min}$ (e/Å$^3$) | 0.16, −0.18 |

orthorhombic space group $P2_12_12_1$ with four molecules in the unit cell. The asymmetric unit in the crystal structure contains only one molecule. The title molecule is composed of a 1-methyl-1*H*-benzo[*d*]imidazole group and a chlorobenzene ring. The benzimidazole and benzene rings of the molecule are not coplanar but rather have a dihedral angle of 42.74(12)°. Furthermore, the dihedral angle between the five- and six-membered rings of the benzimidazole ring system is 0.84(7)°, and the maximum deviation from planarity is 0.0117(31) Å for atom C6, while the crossed torsion angles at the junction, i.e., N1—C2—C7—C6 and N2—C7—C2—C3 are –179.9(3) and 179.0(3)°, respectively.

The imine N1=C1 and amine N2—C1 bond distances in the benzimidazole group [1.330(3) and 1.380(3) Å, respectively] are not equal, with the "imine" length shorter than the "amine" length, as expected. These distances are comparable with those found for (*E*)-1,2-bis(1-methyl-1*H*-benzo[*d*]imidazol-2-yl)ethene [1.3203(18) and 1.3727(17) Å, respectively; [59] and 1,2-bis(1-methyl-1*H*-benzo[*d*]imidazol-2-yl)benzene [1.3133(17)/1.3170(17)

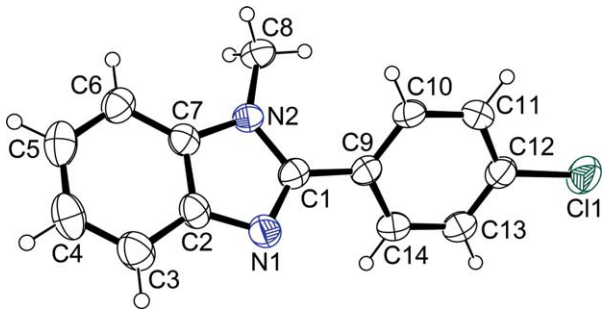


**FIGURE 2.** A view of the title compound showing the atom-numbering scheme. Displacement ellipsoids are drawn at the 40% probability level and H atoms are shown as small spheres of arbitrary radii.
[Color figure can be viewed in the online issue, which is available at wileyonlinelibrary.com.]

**TABLE II**
**Hydrogen bonding geometry for the title compound.**

| D—H···A | D—H (Å) | H···A (Å) | D···A (Å) | D—H···A (°) |
|---|---|---|---|---|
| C13—H13···N1[a] | 0.93 | 2.71 | 3.601(6) | 161 |
| C8—H8A···Cl1[b] | 0.96 | 2.86 | 3.700(4) | 147 |
| C14—H14···Cg1[c] | 0.93 | 2.87 | 3.600(4) | 144 |
| C8—H8B···Cg2[d] | 0.96 | 2.93 | 3.681(3) | 136 |
| C8—H8C···Cg2[e] | 0.96 | 2.80 | 3.541(5) | 134 |

Cg1: the centroid of the C9–C14 ring, Cg2: the centroid of the C2–C7 ring.
[a] $x + 1/2, -y + 1/2, -z$.
[b] $-x, y + 1/2, -z + 1/2$.
[c] $x + 1/2, -y + 1/2, -z$.
[d] $x - 1/2, -y + 3/2, -z$.
[e] $x + 1/2, -y + 3/2, -z$.

and 1.3704(17)/1.3688(17) Å, respectively; [60]. Of the two nitrogen atoms in the benzimidazole ring, only one is methylated, and as a consequence the internal angles at the two nitrogen atoms differ by 2.3(2)°.

Examination of the structure with PLATON [43] reveals that there are no intramolecular interactions in the molecular structure. The crystal structure is stabilized by five weak intermolecular interactions, one of them being a halogen bonding involving the chlorine atom [61] and three of the rest being C—H···Cg($\pi$-ring) contacts. The packing is further stabilized by Van der Waals forces. Full details of the hydrogen bonding geometry are given in Table II.

## INFRARED SPECTRUM

The FTIR spectrum of the title compound is shown in Figure 3. It is well known that the calculated HF and DFT "raw" or "nonscale" harmonic frequencies could significantly overestimate experimental values because of lack of electron correlation, insufficient basis sets and anharmonicity. Much effort has been devoted for accurately reproducing experimental frequencies in theoretical calculations. The HF calculated results are usually more overestimated than the corresponding DFT ones [62]. To compare these, we have calculated the theoretical vibrational spectra of the title compound using both HF and B3LYP method with 6-31G(d) basis set. Frequency calculations at the same levels of theory revealed no imaginary frequencies, indicating that an optimal geometry at these levels of approximation was found for the title compound. We have compared our calculation of the title compound with their experimental results. Theoretical and experimental results of the title compound are shown in Table III. The vibrational bands assignments have been made by using GaussView Molecular Visualization program [50].

The characteristic $\nu$ C—H stretching vibrations of heteroaromatic structure are expected to appear in 3000–3100 $cm^{-1}$ frequency ranges at the IR spectrum. The band observed at 3022 $cm^{-1}$ is attributed to aromatic $\nu$ C=H stretching vibrations of the title compound, which has been calculated with HF and B3LYP at 3022 and 3083 $cm^{-1}$, respectively. The asymmetric and symmetric aliphatic $\nu$ C—H stretching vibrations of the C—$H_3$ group in the 1-position of the benzimidazole ring are at 2950 and 2860 $cm^{-1}$, respectively. These bands have been calculated at 2937 and 2879 $cm^{-1}$ for HF and at 2998 and 2935 $cm^{-1}$ for B3LYP. In addition, the absence of any band $\nu$ N—H in the 3200–3600 $cm^{-1}$ region of the IR spectrum of the compound indicates that *N*-methyl-*o*-phenylenediamine reacted with the $NaHSO_3$ adduct of 4-chlorophenylbenzaldehyde and formed benzimidazole ring system.

Another characteristic regions of the benzimidazole derivatives spectrum are 1500–1650 $cm^{-1}$ which attributed to $\nu$ C=N and $\nu$ C=C stretching vibrations. The title compound shows a strong band at 1600 $cm^{-1}$ which assigned as $\nu$ C=N stretching vibration. This band has been computed as 1626 and 1606 $cm^{-1}$ for HF and B3LYP, respectively. The band observed at 1570 $cm^{-1}$, which can be attributed to the C=C stretching vibration, has been calculated at 1616 $cm^{-1}$ for HF and 1574 $cm^{-1}$ for B3LYP. The IR bands appearing at 1380 and 1249 $cm^{-1}$ are assigned to

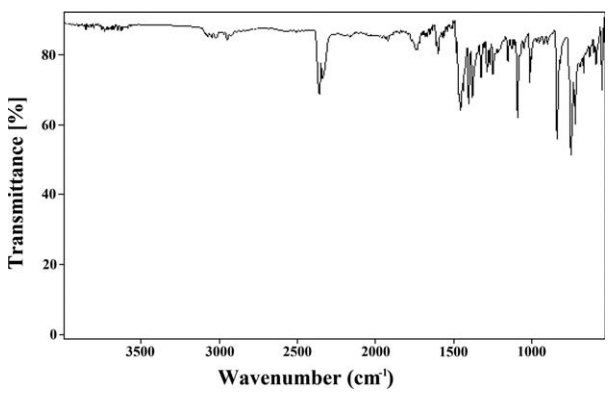


**FIGURE 3.** FTIR spectrum of the title compound.

**TABLE III**

**Comparison of the observed and calculated vibrational spectra of the title compound.**

| Assignments | Experimental IR with KBr ($cm^{-1}$) | Calculated ($cm^{-1}$) | | | |
|---|---|---|---|---|---|
| | | HF/6–31G(d) | | B3LYP/6–31G(d) | |
| | | Scaled freq. | Intensity (km/mol) | Scaled freq. | Intensity (km/mol) |
| $\nu$C—H (R) | 3022 | 3022 | 34.41 | 3083 | 29.43 |
| $\nu_{as}$ C—$H_3$ | 2950 | 2937 | 25.56 | 2998 | 17.38 |
| $\nu_s$ C—$H_3$ | 2860 | 2879 | 45.84 | 2935 | 40.96 |
| $\nu$ C=N | 1600 | 1626 | 29.20 | 1606 | 5.16 |
| $\nu$ C=C (R) | 1570 | 1616 | 17.58 | 1574 | 2.92 |
| $\alpha$C—$H_3$ | 1484 | 1486 | 57.90 | 1482 | 13.93 |
| $\gamma$C—H (R) + $\alpha$ C—$H_3$ | 1457 | 1460 | 45.45 | 1463 | 52.56 |
| $\omega$C—$H_3$ | 1438 | 1442 | 50.42 | 1445 | 32.93 |
| $\nu$C—N | 1380 | 1372 | 62.65 | 1356 | 55.87 |
| $\gamma$ C—H (r) | 1287 | 1294 | 3.97 | 1285 | 8.42 |
| $\nu$C—N | 1249 | 1276 | 26.77 | 1267 | 22.59 |
| $\beta$(R) + $\gamma$ C—H (R) | 1216 | 1228 | 46.02 | 1241 | 10.53 |
| $\gamma$ C—H (r) | 1154 | 1166 | 1.83 | 1168 | 0.89 |
| $\delta$ C—$H_3$ | 1131 | 1126 | 3.82 | 1115 | 0.59 |
| $\nu$ C—Cl | 1092 | 1078 | 76.32 | 1070 | 79.18 |
| $\beta$ (r) | 1014 | 992 | 45.40 | 989 | 47.23 |
| $\omega$ C—H (r) | 839 | 853 | 42.63 | 820 | 29.01 |
| $\delta$ C—H (r) | 818 | 846 | 7.52 | 810 | 3.11 |
| $\omega$ C—H (R) | 751 | 753 | 56.12 | 729 | 54.85 |
| $\beta$ (r) | 723 | 708 | 19.35 | 705 | 14.20 |
| $\beta$ (R) | 534 | 536 | 13.07 | 540 | 8.65 |

Vibrational modes: $\nu$, stretching; s, symmetric; as, asymmetric; $\alpha$, scissoring; $\gamma$, rocking; $\omega$, wagging; $\delta$, twisting; $\beta$, in-plane bending; R, benzimidazole ring; r, benzene ring.

$\nu$ C—N vibrations. These bands have been observed at 1372 and 11276 $cm^{-1}$ for HF and at 1356 and 1267 $cm^{-1}$ for B3LYP in the theoretical spectra of the title compound. All these data agree with those reported in the literature [63, 64].

To make a comparison with experimental observations, we studied the correlation between the calculated and the experimental data (see Fig. 4), and obtained a correlation coefficient of 0.99941 for HF/6-31G(d) and 0.99955 for B3LYP/6-31G(d). According to these results, it is seen that the results of B3LYP method have shown a little better fit to experimental ones than HF in evaluating vibrational frequencies.

## $^1$H AND $^{13}$C NMR SPECTRA

GIAO $^1$H and $^{13}$C chemical shift calculations have been carried out using the HF and B3LYP methods with 6-31G(d) basis set for the optimized geometry. The results of these calculations are tabulated in Table IV. As experimental $^1$H chemical shift values were not available for individual hydrogen atoms of methyl group, we have presented the average of the computed values for methyl hydrogens.

$^1$H NMR results for the compound showed a 1,2-disubstituted benzene system at the ring of the benzimidazole nucleus and a 1,4-disubstituted benzene system because of the 4-chlorophenyl group at the 2-position. H3 and H6 hydrogens appear as two different doublet signals at 7.67 and 7.60 ppm, respectively, which have been calculated at 7.85 and 7.61 ppm for HF and 7.62 and 7.43 ppm for B3LYP. It is concluded that 1,3-tautomerism was prevented by 1-methyl substitution in the benzimidazole ring as reported in the literature [65, 66]. This resulted separate signals for H3 and H6 hydrogens. H4 and H5 protons appear together as multiplet at the region 7.32–7.22 ppm. The two doublets observed at 7.88 and 7.63 ppm are assigned to H10/H14 and H11/H13 protons, respectively, according to influence of chloro group at the 4-position of the 1,4-disubstituted benzene ring. The protons of the methyl group at the 1-position of the benzimidazole ring appear as

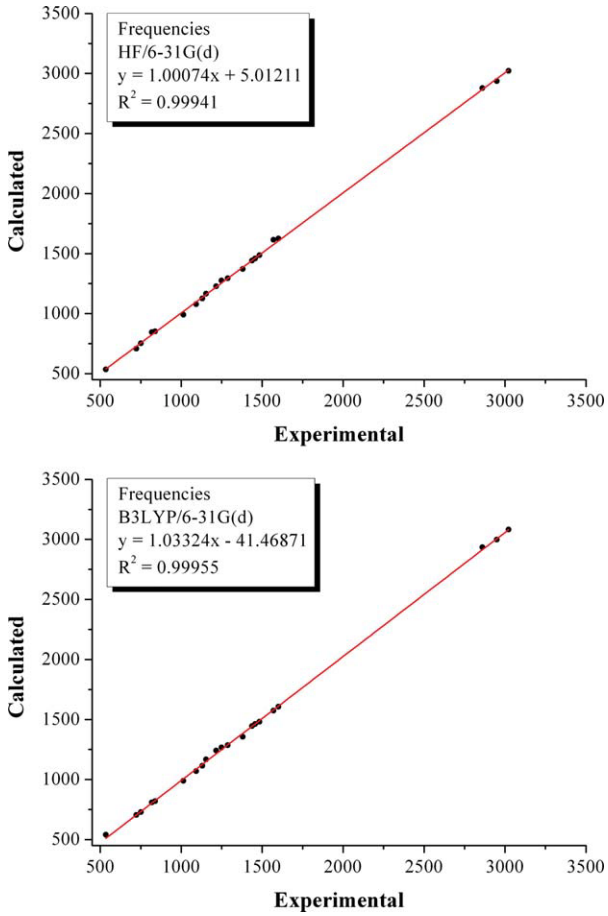


**FIGURE 4.** Correlation graphics of calculated and experimental frequencies of the title compound.[Color figure can be viewed in the online issue, which is available at wileyonlinelibrary.com.]

singlet at 3.92 ppm. This singlet signal has been calculated at 3.36 and 3.71 ppm for HF and B3LYP, respectively.

The experimental $^{13}C$ spectra data also support the structure of the title compound. The carbon of the methylgroup detected at 32.12 ppm that has been calculated at 27.78 ppm for HF and 31.35 ppm for B3LYP. The signal at 152.32 ppm is assigned to C1 carbon next to two nitrogen atoms of benzimidazole ring that indicates the formation of the benzimidazole ring system. This signal has been calculated at 152.54 ppm for HF and 146.23 ppm for B3LYP. As shown in Table IV, all the carbons in the benzimidazole ring appear separately. This observation was thought to arised from preventing 1,3-tautomerism as indicated before. The signals at 119.50, 111.09, 122.53, 123.01, 137.07, and 135.01 ppm are assigned to C3, C6, C4, C5, C2, and C7 carbons, respectively. The carbons of 4-chlorophenyl ring are detected at 131.52, 129.44, 129.21, and 142.83 ppm and assigned as C11/C13, C9, C10/C14, and C12, respectively.

Comparing calculational and the experimental data, we studied the correlation between the calculations and the experiments (see Fig. 5), and obtained a correlation coefficient of 0.99882 for HF/6-31G(d) and 0.99922 for B3LYP/6-31G(d). According to these results, it is seen that the results of B3LYP method have shown better fit to experimental ones than HF in evaluating $^{1}H$ and $^{13}C$ chemical shifts.

## Theoretical Structures

Some selected geometric parameters experimentally obtained and theoretically calculated by HF and B3LYP with 6-31G(d) as the basis set are listed in Table V. It is well known that DFT

**TABLE IV**

**Theoretical and experimental $^{1}H$ and $^{13}C$ isotropic chemical shifts (with respect to TMS, all values in ppm) for the title compound.**

| Atom | Experimental (ppm) (DMSO-$d_6$) | Calculated (ppm) | |
|---|---|---|---|
| | | HF/6–31G(d) | B3LYP/6–31G(d) |
| C1 | 152.32 | 152.54 | 146.23 |
| C2 | 137.07 | 136.11 | 135.44 |
| C3 | 119.50 | 117.53 | 113.33 |
| C4 | 122.53 | 118.18 | 115.92 |
| C5 | 123.01 | 120.72 | 117.21 |
| C6 | 111.09 | 107.49 | 103.81 |
| C7 | 135.01 | 132.14 | 130.45 |
| C8 | 32.12 | 27.78 | 31.35 |
| C9 | 129.44 | 126.28 | 123.07 |
| C10 | 129.21 | 127.8 | 122.92 |
| C11 | 131.52 | 124.6 | 121.99 |
| C12 | 142.83 | 135.44 | 136.82 |
| C13 | 131.52 | 125.83 | 123.06 |
| C14 | 129.21 | 129.71 | 125.74 |
| H3 | 7.67 (d) | 7.85 | 7.62 |
| H4 | 7.22 (m) | 7.44 | 7.39 |
| H5 | 7.32 (m) | 7.57 | 7.41 |
| H6 | 7.60 (d) | 7.61 | 7.43 |
| H8 | 3.92 (s) | 3.36[a] | 3.71[a] |
| H10 | 7.88 (d) | 7.73 | 7.51 |
| H11 | 7.63 (d) | 7.65 | 7.45 |
| H13 | 7.63 (d) | 7.64 | 7.45 |
| H14 | 7.88 (d) | 8.19 | 8.09 |

[a] Average.

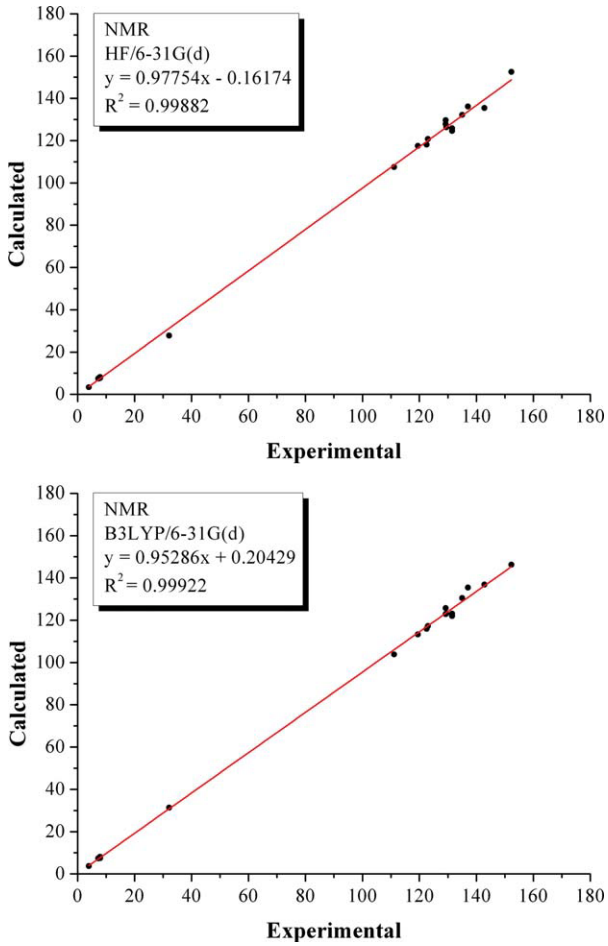


**FIGURE 5.** Correlation graphics of calculated and experimental NMR chemical shift values of the title compound.[Color figure can be viewed in the online issue, which is available at wileyonlinelibrary.com.]

optimized bond lengths are usually longer and more accurate than HF, because of inclusion of electron correlation. However, according to our calculations, HF method correlates well for the bond lengths compared with the other method (Table V). Although the largest difference between experimental and calculated bond lengths is about 0.042 Å for HF and 0.026 Å for B3LYP, the root mean square error (RMSE) is found about 0.013 Å for HF and 0.015 Å for B3LYP, indicating that the bond lengths obtained by HF method show the strongest correlation with the experimental values. The same trend was not observed in bond angles. This time, the largest difference for the bond angles obtained by HF method is smaller than that of B3LYP, but the RMS error is not.

When the X-ray structure of the title compound is compared with its optimized counterparts (see Fig. 6), slight conformational discrepancies are observed between them. The dihedral angle between the benzimidazole and benzene rings of the title molecule is calculated at 42.147° for HF and at 33.836° for B3LYP, whereas the dihedral angle between the five- and six-membered rings of the benzimidazole ring system is calculated at 0.061° and 0.238° for HF and B3LYP, respectively.

A logical method for globally comparing the structures obtained with the theoretical calculations is by superimposing the molecular skeleton with that obtained from X-ray diffraction, giving an RMSE of 0.064 Å for HF/6-31G(d) and 0.113 Å for B3LYP/6-31G(d) calculations (see Fig. 6). Consequently, HF method correlates well for the geometrical parameters when compared with B3LYP.

## TOTAL ENERGIES AND DIPOL MOMENTS

To investigate the total energy and dipole moment behavior of the title compound in solvent media, we have carried out optimization calculations in three solvents (chloroform, methanol, water) at the B3LYP/6-31G(d) level using Onsager and PCM methods and the results are given in Table VI.

As can be seen from Table VI, the obtained total energies of the title compound by Onsager and PCM models decrease with the increasing polarity of the solvent so that the stability of the title compound increases. The energy difference between gas phase and solvent media was found to be significant for both methods. The PCM method supplied more stable structure than Onsager's method with the increasing polarity of the solvent. The trend in the total energies is also observed in the dipole moments. The dipole moments calculated by PCM method are larger than those of Onsager method in different solvents, and the dipole moments obtained for two solvation methods increase with the increase of the solvent polarity.

## MOLECULAR ELECTROSTATIC POTENTIAL

Molecular electrostatic potential, $V(\boldsymbol{r})$, at a given point $r(x, y, z)$ in the vicinity of a molecule, is defined in terms of the interaction energy between the electrical charge generated from the molecule electrons and nuclei and a positive test charge (a proton) located at $\boldsymbol{r}$. For the system studied the $V(\boldsymbol{r})$ values were calculated as described previously using the equation [67],

**TABLE V**

**Optimized and experimental geometries of the title compound in the ground state.**

| Parameters | Experimental | Calculated [6–31G(d)] | | Parameters | Experimental | Calculated [6–31G(d)] | |
|---|---|---|---|---|---|---|---|
| Bond lengths (Å) | | HF | B3LYP | N2—C7—C6 | 131.6(3) | 132.23905 | 132.16968 |
| Cl1—C12 | 1.739(3) | 1.74193 | 1.75732 | N2—C1—C9 | 124.2(2) | 123.91944 | 124.57053 |
| N1—C1 | 1.330(3) | 1.28800 | 1.31857 | C1—N1—C2 | 104.3(3) | 105.53552 | 105.48905 |
| N1—C2 | 1.384(4) | 1.37792 | 1.38078 | C1—N2—C7 | 106.6(2) | 105.74673 | 106.12226 |
| N2—C1 | 1.380(3) | 1.37224 | 1.39270 | C1—N2—C8 | 128.1(2) | 129.25014 | 129.14814 |
| N2—C7 | 1.375(4) | 1.37981 | 1.38636 | C7—N2—C8 | 124.7(2) | 124.33113 | 124.11806 |
| N2—C8 | 1.460(3) | 1.44689 | 1.45356 | C1—C9—C10 | 122.5(3) | 122.23687 | 123.24874 |
| C1—C9 | 1.461(4) | 1.48017 | 1.47138 | C1—C9—C14 | 119.5(3) | 118.78023 | 118.19825 |
| C2—C3 | 1.402(4) | 1.39229 | 1.40148 | C2—C3—C4 | 118.0(3) | 117.96023 | 118.02772 |
| C2—C7 | 1.391(4) | 1.39152 | 1.41457 | C2—C7—C6 | 122.7(3) | 122.29894 | 122.42980 |
| C3—C4 | 1.374(5) | 1.37789 | 1.39047 | C3—C4—C5 | 121.7(3) | 121.18896 | 121.35898 |
| C4—C5 | 1.386(5) | 1.40203 | 1.41013 | C3—C2—C7 | 119.3(3) | 120.24467 | 119.89022 |
| C5—C6 | 1.376(5) | 1.37923 | 1.39289 | C4—C5—C6 | 121.6(3) | 121.48601 | 121.54587 |
| C6—C7 | 1.390(4) | 1.39052 | 1.39715 | C5—C6—C7 | 116.7(3) | 116.82051 | 116.74658 |
| C9—C10 | 1.390(4) | 1.38982 | 1.40419 | C9—C10—C11 | 121.5(3) | 120.82206 | 120.97254 |
| C9—C14 | 1.389(4) | 1.39129 | 1.40575 | C9—C14—C13 | 121.3(3) | 120.74342 | 121.03353 |
| C10—C11 | 1.379(4) | 1.38457 | 1.39430 | C10—C11—C12 | 118.9(3) | 119.19496 | 119.24378 |
| C11—C12 | 1.378(5) | 1.38166 | 1.39319 | C10—C9—C14 | 117.9(3) | 118.91896 | 118.49474 |
| C12—C13 | 1.370(5) | 1.38398 | 1.39593 | C11—C12—C13 | 121.2(3) | 121.00761 | 120.98030 |
| C13—C14 | 1.379(5) | 1.38205 | 1.39055 | C12—C13—C14 | 119.3(3) | 119.30255 | 119.25882 |
| RMSE[a] | | 0.01270 | 0.01524 | RMSE[a] | | 0.62766 | 0.55195 |
| Max. difference [a] | | 0.04200 | 0.02593 | Max. difference[a] | | 1.23552 | 1.30175 |
| Bond angles (°) | | | | Torsion angles (°) | | | |
| Cl1—C12—C11 | 119.5(3) | 119.47621 | 119.48424 | N1—C2—C7—C6 | 179.9(3) | 179.85883 | 179.58906 |
| Cl1—C12—C13 | 119.2(3) | 119.51542 | 119.53423 | N1—C1—C9—C10 | −134.4(3) | −136.19093 | −144.67071 |
| N1—C1—N2 | 112.6(3) | 113.50417 | 112.82572 | N1—C1—C9—C14 | 41.1(5) | 40.86795 | 32.50768 |
| N1—C2—C3 | 129.8(3) | 130.00385 | 129.94670 | N2—C7—C2—C3 | 179.0(3) | −179.98638 | −179.82246 |
| N1—C2—C7 | 110.9(2) | 109.75128 | 110.16301 | N2—C1—C9—C10 | 42.5(5) | 43.31932 | 35.20312 |
| N1—C1—C9 | 123.1(3) | 122.57480 | 122.60365 | N2—C1—C9—C14 | −142.0(3) | −139.62180 | −147.61850 |
| N2—C7—C2 | 105.6(2) | 105.46111 | 105.39810 | | | | |

[a] RMSE and maximum differences between the bond lengths and angles computed by the theoretical methods and those obtained from X-ray diffraction.

$$V(r) = \sum_A \frac{Z_A}{|R_A - r|} - \int \frac{\rho(r')}{|r' - r|} dr'$$

where $Z_A$ is the charge of nucleus A, located at $\boldsymbol{R}_A$, $\rho(\boldsymbol{r}')$ is the electronic density function of the molecule, and $\boldsymbol{r}'$ is the dummy integration variable.

Molecular electrostatic potential (MEP) is related to the electronic density and is a very useful descriptor in understanding sites for electrophilic attack and nucleophilic reactions as well as hydrogen bonding interactions [68–70]. The electrostatic potential is not always reliable for electrophilic and nucleophilic attack, but is more reliable for approach and thus noncovalent interactions [71]. The electrostatic potential $V(\boldsymbol{r})$ are also well suited for analyzing processes based on the "recognition" of one molecule by another, as in drug-receptor and enzyme-substrate interactions, because it is through their potentials that the two species first see each other [72, 73]. It should be emphasized that $V(\boldsymbol{r})$ is a real physical property, an observable, which can be determined experimentally, by diffraction techniques, as well as computationally [74].

To predict reactive sites for electrophilic and nucleophilic attack for the title molecule, MEP was calculated at the B3LYP/6-31G(d) optimized geometry. The negative (red color) regions of MEP were related to electrophilic reactivity and the positive (blue color) ones to nucleophilic reactivity shown in Figure 7. As can be seen in Figure 7, there is one possible site on the title compound for electrophilic attack. The negative region is localized on the nitrogen atom of the imidazole ring, N1, with a maximum value of −0.052 a.u.

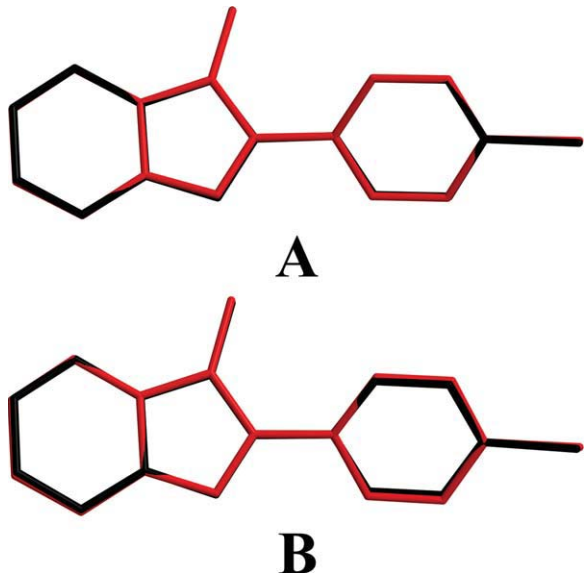


**FIGURE 6.** Atom-by-atom superimposition of the structures calculated (red) [A = HF/6-31G(d), B = B3LYP/6-31G(d)] over the X-ray structure (black) for the title compound. Hydrogen atoms omitted for clarity. [Color figure can be viewed in the online issue, which is available at wileyonlinelibrary.com.]

However, a maximum positive region is associated with the methyl H atoms indicating a possible site for nucleophilic attack with a maximum value of 0.032 a.u. These results supply information about the region from where the compound can have intermolecular interaction and metallic bonding. So, Figure 7 confirms the existence of weak intermolecular interactions observed in the solid state.

## FRONTIER MOLECULAR ORBITALS ANALYSIS

The frontier molecular orbitals play an important role in the electric and optical properties, as well as in UV–Vis spectra and chemical reactions [75]. Figure 8 shows the distributions and energy levels of the HOMO − 1, HOMO, LUMO, and LUMO +1 orbitals computed at the B3LYP/6-31G(d) level for the title compound.

As seen from Figure 8, both the highest occupied molecular orbital (HOMO) and the lowest-lying unoccupied molecular orbital (LUMO) are mainly delocalized among all the atoms. However, the HOMO − 1 and LUMO +1 orbitals are partially localized on the different parts of the title molecule. The HOMO − 1 orbitals are delocalized on the benzimidazole ring, while the LUMO +1 orbitals are delocalized on the benzene ring. Both of the highest occupied molecular orbitals (HOMOs) and the lowest unoccupied molecular orbitals (LUMOs) are mostly the $\pi$-antibonding type orbitals. The value of the energy separation between the HOMO and LUMO is 4.595 eV and this large energy gap indicates that the title structure is quite stable.

**TABLE VI**

**Total energies and dipole moments of the title compound in different solvent.**

| Method | $\varepsilon$ | Energy (a.u.) | $\Delta E$ (kcal/mol) | $\mu$ (Debye) |
|---|---|---|---|---|
| B3LYP | 1 | −1109.83453151 | | 3.4267 |
| Onsager | 4.90 | −1109.83531660 | −0.493 | 3.9378 |
| | 32.63 | −1109.83562276 | −0.685 | 4.1467 |
| | 78.39 | −1109.83565941 | −0.708 | 4.1722 |
| PCM | 4.90 | −1109.84417398 | −6.051 | 4.3482 |
| | 32.63 | −1109.84844018 | −8.728 | 4.8036 |
| | 78.39 | −1109.84913408 | −9.163 | 4.8812 |

$\Delta E = E_{Solvation} - E_{Gas}$; $\varepsilon$ = dielectric constant.

## NONLINEAR OPTICAL PROPERTY CALCULATIONS

Nonlinear optics (NLO) is at the forefront of current research because of its importance in providing the key functions of frequency shifting, optical modulation, optical switching, optical logic, and optical memory for the emerging technologies in areas, such as telecommunications, signal processing and optical interconnections [76–79]. Benzimidazole itself crystallizes in a noncentrosymmetric

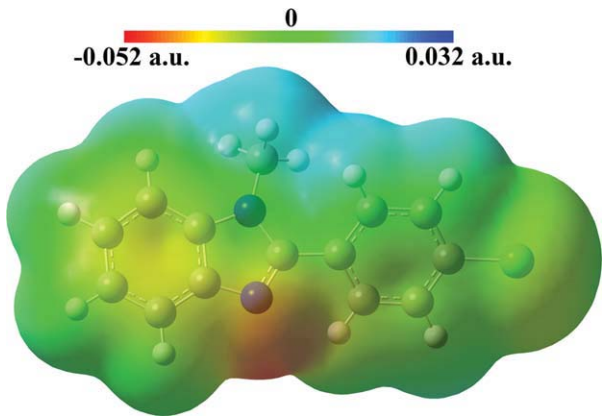


**FIGURE 7.** Molecular electrostatic potential (MEP) map plotted on the surface of the title compound with an isodensity value of 0.0004 a.u. calculated at the B3LYP/6-31G(d) level.[Color figure can be viewed in the online issue, which is available at wileyonlinelibrary.com.]

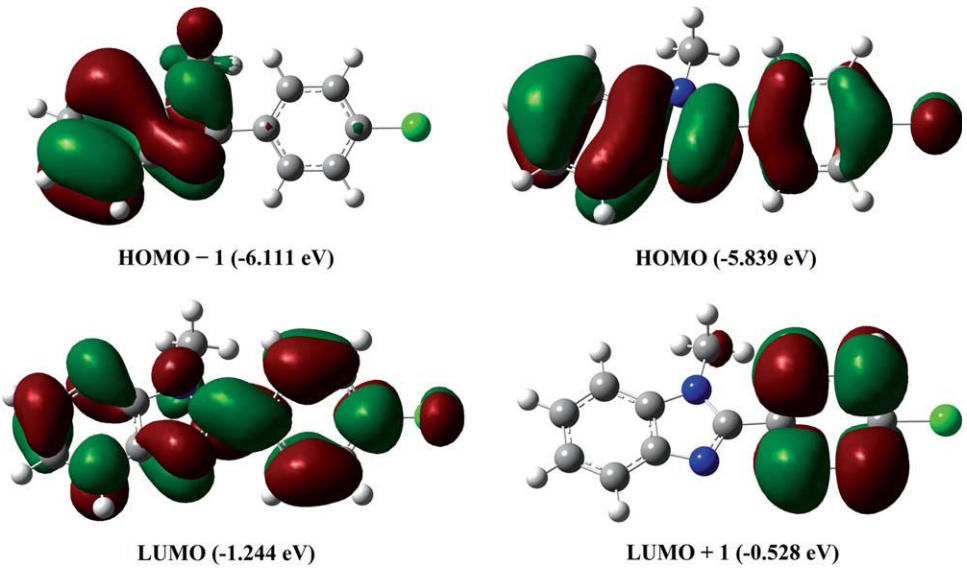


**FIGURE 8.** Molecular orbital surfaces and energy levels given in parentheses for the HOMO − 1, HOMO, LUMO and LUMO +1 of the title compound computed at B3LYP/6-31G(d) level. The positive phase is red, and the negative phase is green.[Color figure can be viewed in the online issue, which is available at wileyonlinelibrary.com.]

space group and is of interest as a potential nonlinear optical material [80].

The calculations of the mean linear polarizability ($\alpha$) and the mean first hyperpolarizability ($\beta$) from the Gaussian output have been explained in detail previously [81], and DFT has been extensively used as an effective method to investigate the organic NLO materials [82]. In this work, the nonlinear optical properties of the title compound were calculated at the B3LYP/6-31G(d) level according to the reference method [83]. The calculated values of $\alpha$ and $\beta$ for the title compound are 26.703 $Å^3$ and 45.3402 $\times$ $10^{-31}$ $cm^5$/esu, which are greater than those of urea (the $\alpha$ and $\beta$ of urea are 3.8312 $Å^3$ and 3.7289 $\times$ $10^{-31}$ $cm^5$/esu calculated with the same method) [84]. Although the calculated value of $\alpha$ is greater than that of *para*-nitroaniline, the value of $\beta$ is smaller (the $\alpha$ and $\beta$ of *para*-nitroaniline are 12.7176 $Å^3$ and 114.9189 $\times$ $10^{-31}$ $cm^5$/esu calculated with the same method). This indicates that the title compound is a good candidate as second-order nonlinear optical material.

## Conclusions

In this study, we have synthesized a novel benzimidazole compound, $C_{14}H_{11}ClN_2$, and characterized by spectroscopic (FTIR and NMR) and structural (XRD) techniques. For the geometrical parameters, the results of HF method have shown a better fit to experimental ones than those of B3LYP method. However, it is seen from the theoretical results that the B3LYP method seems to be more appropriate than HF method for the calculation of vibrational frequencies and chemical shifts. It was noted here that the experimental results belong to solid phase and theoretical calculations belong to gaseous phase. In the solid state, the existence of the crystal field along with the intermolecular interactions have connected the molecules together, which result in the differences of bond parameters between the calculated and experimental values. Despite the differences observed in the geometric parameters, the general agreement is good and the theoretical calculations support the solid-state structures. The MEP map agrees well with the solid-state interactions. The total energy of the title compound decrease with the increasing polarity of the solvent and the stability of the title compound increase in going from the gas phase to the solution phase. The computed NLO properties of the title compound are much greater than those of urea, so the title compound is a good candidate as second-order nonlinear optical material.

## References


1. O'Niel, M. J.; Smith, M.; Heckelman, P. E., Eds. The Merck Index, 13th ed.; Merck & Co. Inc.; New Jersey, 2001; p 10074; P-1785, Monograph Number.
2. Ayhan-Kılcıgil, G.; Kuş, C.; Özdamar, E. D.; Can-Eke, B.; İşcan, M. Arch Pharm 2007, 340, 607.
3. Kuş, C.; Ayhan-Kılcıgil, G.; Can-Eke, B.; İşcan, M. Arch Pharm Res 2004, 27, 156.
4. Ateş-Alagöz, Z.; Kuş, C.; Çoban, T. J Enzyme Inhib Med Chem 2005, 20, 325.
5. Navarrete-Vázquez, G.; Cedillo, R.; Hernández-Campos, A.; Yépez, L.; Hernández-Luis, F.; Valdez, J.; Morales, R.; Cortés, R.; Hernández, M.; Castillo, R. Bioorg Med Chem Lett 2001, 11, 187.
6. Katiyar, S. K.; Gordon, V. R.; McLaughlin, G. L.; Edlind, T. D. Antimicrob Agents Chemother 1994, 38, 2086.
7. Ravina, E.; Sanchez-Alonso, R.; Fueyo, J.; Baltar, M. P.; Bos, J.; Iglesias, R.; Sanmartin, M. L. Arzneim-Forsch/Drug Res 1993, 43, 684.
8. Garuti, L.; Roberti, M.; Malagoli, M.; Rossi, T.; Castelli, M. Bioorg Med Chem Lett 2000, 10, 2193.
9. Rao, A.; Chimirri, A.; De Clercq, E.; Monforte, A. M.; Monforte, P.; Pannecouque, C.; Zappalá, M. Il Farmaco 2002, 57, 819.
10. Chimirri, A.; De Sarro, A.; De Sarro, G.; Gitto, R.; Zappalá, M. Il Farmaco 2001, 56, 821.
11. Thakurdesai, P. A.; Wadodkar, S. G.; Chopade, C. T. Pharm Online 2007, 1, 314.
12. Le, H. T.; Lemaire, I. B.; Gilbert, A. K.; Jolicoeur, F.; Yang, L.; Leduc, N.; Lemaire, S. J Pharmacol Exp Ther 2004, 309, 146.
13. Lackner, T. E.; Clissold, S. P. Drugs 1989, 38, 204.
14. Ersan, S.; Nacak, S.; Noyanalpan, N.; Yeşilada, E. Arzneim-Forsch/Drug Res 1997, 47, 834.
15. Serafin, B.; Borkowska, G.; Glowczyk, J.; Kowalska, I.; Rump, S. Pol J Pharmacol Pharm 1989, 41, 89.
16. Kubo, K.; Inada, Y.; Kohara, Y.; Sugiura, Y.; Ojima, M.; Itoh, K.; Furukawa, Y.; Nishikawa, Y. K.; Naka, T. J Med Chem 1993, 36, 1772.
17. Abdel-monem Abdel-hafez, A. Arch Pharm Res 2007, 30, 678.
18. Ram, S.; Wise, D. S.; Wotring, L. L.; McCall, J. W.; Townsend, L. B. J Med Chem 1992, 35, 539.
19. Mavrova, A. Ts.; Denkova, P.; Tsenov, Y. A.; Anichina, K. K.; Vutchev, D. I. Bioorg Med Chem 2007, 15, 6291.
20. Ayhan-Kılcıgil, G.; Altanlar, N. Il Farmaco 2003, 58, 1345.
21. Özden, S.; Atabey, D.; Yıldız, S.; Göker, H. Bioorg Med Chem 2005, 13, 1587.
22. Terzioglu, N.; van Rijn, R. M.; Bakker, R. A.; de Esch, I. J. P.; Leurs, R. Bioorg Med Chem Lett 2004, 14, 5251.
23. Küçükbay, H.; Durmaz, R.; Orhan, E.; Günal, S. Il Farmaco 2003, 58, 431.
24. Agh-Atabay, N. M.; Dulger, B.; Gucin, F. Eur J Med Chem 2003, 38, 875.
25. Andrzejewska, M.; Yépez-Mulia, L.; Cedillo-Rivera, R.; Tapia, A.; Vilpo, L.; Vilpo, J.; Kazimierczuk, Z. Eur J Med Chem 2002, 37, 973.
26. Castilo-Blum, S. E.; Barba-Behrens, N. Coord Chem Rev 2003, 196, 3.
27. Monthilal, K. K.; Karunakaran, C.; Rajendran, A.; Murugesan, R. J Inorg Biochem 2004, 98, 322.
28. Wright, J. B. Chem Rev 1951, 48, 397.
29. Preston, P. N. Chem Rev 1974, 74, 279.
30. Chen, C. -L.; Goforth, A. M.; Smith, M. D.; Su, C. -Y.; zur Loye, H. C. Inorg Chem 2005, 44, 8762.
31. Zheng, X.-L.; Liu, Y.; Pan, M.; Lü, X.-Q.; Zhang, J. -Y.; Zhao, C.-Y.; Tong, Y.-X.; Su, C.-Y. Angew Chem Int Ed Engl 2007, 46, 7399.
32. Qi, D.-Q.; Hou, G.-G.; Ma, J.-P.; Huang, R.-Q.; Dong, Y.-B. Acta Cryst 2009, C65, o85.
33. Herrmann, W. A. Angew Chem Int Ed Engl 2002, 41, 1290.
34. Mohan, S.; Sundaraganesan, N. Spectrochim Acta Part A 1991, 47, 1111.
35. Klots, T. D.; Devlin, P.; Collier, W. B. Spectrochim Acta Part A 1997, 53, 2445.
36. Morsy, M. A.; Al-Khaldi, M. A.; Suwaiyan, A. J Phys Chem A 2002, 106, 9196.
37. Yurdakul, Ş.; Yılmaz, C. Vib Spectrosc 1999, 21, 127.
38. Ridley, H. F.; Spickett, R. G. W.; Timmis, G. M. J Heterocycl Chem 1965, 2, 453.
39. Sheldrick, G. M. SHELXS-97 Program for the Solution of Crystal Structures. University of Göttingen, Germany, 1997.
40. Farrugia, L. J. J Appl Cryst 1999, 30, 837.
41. Sheldrick, G. M. SHELXL-97 Program for Crystal Structures Refinement. University of Göttingen, Germany, 1997.
42. Stoe & Cie. X-AREA (Version 1.18) and X-RED32 (Version 1.04). Stoe & Cie: Darmstadt, Germany, 2002.
43. Spek, A. L. J Appl Cryst 2003, 36, 7.
44. Lee, C.; Yang, W.; Parr, R. G. Phys Rev B 1988, 37, 785.
45. Becke, A. D. J Chem Phys 1993, 98, 5648.
46. Ditchfield, R.; Hehre, W. J.; Pople, J. A. J Chem Phys 1971, 54, 724.
47. Foresman, J. B.; Frisch, A. Exploring Chemistry with Electronic Structure Methods, 2nd ed.; Gaussian, Inc.: Pittsburgh, PA, 1996.
48. Ditchfield, R. J Chem Phys 1972, 56, 5688.
49. Wolinski, K.; Hinton, J. F.; Pulay, P. J Am Chem Soc 1990, 112, 8251.
50. Dennington, R., II; Keith, T.; Millam, J. GaussView (Version 4.1.2). Semichem, Inc., Shawnee Mission: KS, 2007.
51. Frisch, M. J.; Trucks, G. W.; Schlegel, H. B.; Scuseria, G. E.; Robb, M. A.; Cheeseman, J. R.; Montgomery, J. A.; Vreven, T., Jr.; Kudin, K. N.; Burant, J. C.; Millam, J. M.; Iyengar, S. S.; Tomasi, J.; Barone, V.; Mennucci, B.; Cossi, M.; Scalmani, G.; Rega, N.; Petersson, G. A.; Nakatsuji, H.; Hada, M.; Ehara, M.; Toyota, K.; Fukuda, R.; Hasegawa, J.; Ishida, M.; Nakajima, T.; Honda, Y.; Kitao, O.; Nakai, H.; Klene, M.; Li, X.; Knox, J. E.; Hratchian, H. P.; Cross, J. B.; Adamo, C.; Jaramillo, J.; Gomperts, R.; Stratmann, R. E.; Yazyev, O.; Austin, A. J.; Cammi, R.; Pomelli, C.; Ochterski, J. W.; Ayala, P. Y.; Morokuma, K.; Voth, G. A.; Salvador, P.; Dannenberg, J. J.; Zakrzewski, V. G.; Dapprich, S.; Daniels, A. D.; Strain, M. C.; Farkas, O.; Malick, D. K.; Rabuck, A. D.; Raghavachari, K.; Foresman, J. B.; Ortiz, J. V.; Cui, Q.; Baboul, A. G.; Clifford, S.; Cioslowski, J.;

Stefanov, B. B.; Liu, G.; Liashenko, A.; Piskorz, P.; Komaromi, I.; Martin, R. L.; Fox, D. J.; Keith, T.; Al-Laham, M. A.; Peng, C. Y.; Nanayakkara, A.; Challacombe, M.; Gill, P. M. W.; Johnson, B.; Chen, W.; Wong, M. W.; Gonzalez, C.; Pople, J. A. Gaussian 03 (Revision E. 01). Gaussian, Inc.: Wallingford, CT, 2004.

52. Cancès, E.; Mennucci, B.; Tomasi, J. J Chem Phys 1997, 107, 3032.
53. Onsager, L. J Am Chem Soc 1936, 58, 1486.
54. Miertus, S.; Scrocco, E.; Tomasi, J. Chem Phys 1981, 55, 117.
55. Barone, V.; Cossi, M. J Phys Chem A 1998, 102, 1995.
56. Cossi, M.; Rega, N.; Scalmani, G.; Barone, V. J Comput Chem 2003, 24, 669.
57. Tomasi, J.; Mennucci, B.; Cammi, R. Chem Rev 2005, 105, 2999.
58. Farrugia, L. J. J Appl Cryst 1997, 30, 565.
59. Stibrany, R. T.; Schugar, H. J.; Potenza, J. A. Acta Cryst 2005, C61, o354.
60. Gilbert, J. G.; Addison, A. W.; Prabakaran, P.; Butcher, R. J.; Bocelli, G. Inorg Chem Commun 2004, 7, 701.
61. Politzer, P.; Murray, J. S.; Concha, M. C. J Mol Model 2007, 13, 643.
62. Zhou, W.; Lu, J.; Zhang, Z.; Zhang, Y.; Cao, Y.; Lu, L.; Yang, X. Vibr Spectrosc 2004, 34, 199.
63. Infante-Castillo, R.; Rivera-Montalvo, L. A.; Hernández-Rivera S. P. J Mol Struct 2008, 877, 10.
64. Sundaraganesan, N.; Ilakiamani, S.; Subramani, P.; Joshua, B. D. Spectrochim Acta Part A 2007, 67, 628.
65. Sridharan, V.; Saravanan, S.; Muthusubramanian, S.; Sivasubramanian, S. Magn Reson Chem 2005, 43, 551.
66. Begtrup, M.; Claramunt, R. M.; Elguero, J. J Chem Soc Perkin Trans 1978, 2, 99.
67. Politzer, P.; Murray, J. S. Theor Chem Acc 2002, 108, 134.
68. Scrocco, E.; Tomasi, J. Adv Quantum Chem 1978, 11, 115.
69. Luque, F. J.; López, J. M.; Orozco, M. Theor Chem Acc 2000, 103, 343.
70. Okulik, N.; Jubert, A. H. Internet Electron. J Mol Des 2005, 4, 17.
71. Politzer, P.; Murray, J. S.; Concha, M. C. Int J Quantum Chem 2002, 88, 19.
72. Politzer, P.; Laurence, P. R.; Jayasuriya, K. Env Health Perspect 1985, 61, 191.
73. Scrocco, E.; Tomasi, J. In Topics in Current Chemistry; Springer-Verlag: Berlin, 1973; Vol. 42, p 95.
74. Politzer, P.; Truhlar, D. G., Eds. Chemical Applications of Atomic and Molecular Electrostatic Potentials; Plenum Press: New York, 1981.
75. Fleming, I. Frontier Orbitals and Organic Chemical Reactions; John Wiley: London, 1976.
76. Andraud, C.; Brotin, T.; Garcia, C.; Pellé, F.; Goldner, P.; Bigot, B.; Collet, A. J Am Chem Soc 1994, 116, 2094.
77. Geskin, V. M.; Lambert, C.; Brédas, J.-L. J Am Chem Soc 2003, 125, 15651–15658.
78. Nakano, M.; Fujita, H.; Takahata, M.; Yamaguchi, K. J Am Chem Soc 2002, 124, 9648.
79. Sajan, D.; Joe, H.; Jayakumar, V. S.; Zaleski, J. J Mol Struct 2006, 785, 43.
80. Vijayan, N.; Bhagavannarayana, G.; Kanagasekaran, T.; Ramesh Babu, R.; Gopalakrishnan, R.; Ramasamy, P. Cryst Res Technol 2006, 41, 784.
81. Thanthiriwatte, K. S.; Nalin de Silva, K. M. J Mol Struct (Theochem) 2002, 617, 169.
82. Sun, Y.-X.; Hao, Q.-L.; Wei, W.-X.; Yu, Z.-X.; Lu, L.-D.; Wang, X.; Wang, Y.-S. J Mol Struct (Theochem) 2009, 904, 74.
83. de Silva, I. C.; de Silva, R. M.; de Silva, K. M. N. J Mol Struct (Theochem) 2005, 728, 141.
84. Sun, Y.-X.; Hao, Q.-L.; Wei, W.-X.; Yu, Z.-X.; Lu, L.-D.; Wang, X.; Wang, Y. -S. J Mol Struct 2009, 929, 10.